# p50 Nuclear Factor-κB Overexpression in Tumor-Associated Macrophages Inhibits M1 Inflammatory Responses and Antitumor Resistance

Alessandra Saccani,[1] Tiziana Schioppa,[1] Chiara Porta,[4] Subhra K. Biswas,[1] Manuela Nebuloni,[3] Luca Vago,[3] Barbara Bottazzi,[4] Mario P. Colombo,[5] Alberto Mantovani,[2,4] and Antonio Sica[4]

[1]Istituto di Ricerche Farmacologiche Mario Negri; [2]Institute of General Pathology; [3]Institute of Pathology, Department of Clinical Sciences L. Sacco, State University of Milan; [4]IRCCS Istituto Clinico Humanitas; and [5]Immunotherapy and Gene Therapy Unit, Istituto Nazionale Tumori, Milan, Italy

## Abstract

**Tumor-associated macrophages (TAM) are a major inflammatory infiltrate in tumors and a major component of the protumor function of inflammation. TAM in established tumors generally have an M2 phenotype with defective production of interleukin-12 (IL-12) and high IL-10. Here, we report that defective responsiveness of TAM from a murine fibrosarcoma and human ovarian carcinoma to M1 activation signals was associated with a massive nuclear localization of the p50 nuclear factor-κB (NF-κB) inhibitory homodimer. p50 overexpression inhibited IL-12 expression in normal macrophages. TAM isolated from $p50^{-/-}$ mice showed normal production of M1 cytokines, associated with reduced growth of transplanted tumors. Bone marrow chimeras showed that p50 inactivation in hematopoietic cells was sufficient to result in reduced tumor growth. Thus, p50 NF-κB overexpression accounts for the inability of TAM to mount an effective M1 antitumor response capable of inhibiting tumor growth.** (Cancer Res 2006; 66(23): 11432-40)

## Introduction

The presence of inflammatory cells in solid tumors, along with epidemiologic evidence, has long suggested that cancers arise at sites of chronic inflammation (1–3). This hypothesis has recently received molecular confirmations in inflammation-associated cancer models (4–6), which provide *in vivo* evidence supporting a causal relationship between nuclear factor-κB (NF-κB)–mediated inflammation and tumorigenesis. In this context, tumor-associated macrophages (TAM) represent the major inflammatory component of the tumor infiltrate and are considered prominent part of the inflammatory circuits that promote tumor progression (7). TAMs are recruited at the tumor site by tumor-derived chemotactic factor for monocytes, later identified as the chemokine CCL2/MCP-1 (7–10). These cells have a dual function in their interaction with neoplastic cells, as they can express activities that can prevent the establishment and spread of tumor cells and, simultaneously, have functions to support tumor growth and dissemination (1, 3, 7, 11). This ambivalent relationship reflects the elevated functional plasticity of macrophages, able to express different functional programs in response to different microenvironmental signals, as exemplified in the M1-M2 paradigm of macrophage polarization (7, 12–16). M1 macrophages are potent effector cells that kill microorganisms and tumor cells and produce copious amounts of proinflammatory cytokines. In contrast, M2 macrophages tune inflammatory responses and adaptive Th1 immunity, scavenge debris, and promote angiogenesis, tissue remodeling, and repair (15). The M1/M2 dichotomy of macrophage polarization is illustrated in TAMs, which can elicit both protumoral and antitumoral activities, as previously suggested in the "macrophage balance hypothesis" (11). During tumor progression, TAMs acquire a skewed M2 phenotype and express protumoral functions (7).

We have previously reported that TAMs from both murine and human tumors express defective interleukin-12 (IL-12) production and NF-κB activity, along with high level of the immunosuppressive cytokine IL-10 (17), and speculated that this molecular pathway may underlie other alterations of TAM functions dependent on NF-κB activation (7). The NF-κB family is a key player in controlling both innate and adaptive immunity (18). NF-κB proteins are present in the cytoplasm in association with inhibitory proteins that are known as inhibitors of NF-κB (IκBs). After activation by different stimuli, the IκB proteins become phosphorylated, ubiquitylated, and, subsequently, degraded by the proteasome (18). The degradation of IκB allows NF-κB proteins to translocate to the nucleus and bind their cognate DNA-binding sites to regulate the transcription of a large number of genes, including antimicrobial peptides, cytokines, chemokines, stress response proteins, and antiapoptotic proteins. The mammalian NF-κB family include RELA (p65), NF-κB1 (p50 and p105), NF-κB2 (p52 and p100), c-REL, and RELB (18). Unlike the c-REL, RELB, and RELA proteins, p50 and p52 do not contain the COOH-terminal transactivation domain and may form inhibitory homodimers able to bind NF-κB consensus sequences and to function as transcriptional repressors (18). Altered expression and activation of NF-κB family members in immunocompetent cells has been reported in various pathologic situations. Although its constitutive activation is associated with chronic inflammatory diseases (19), defective NF-κB activity has been reported in other pathologies, such as cancer and sepsis (19–21).

Here, we provide evidence that TAMs are characterized by a status of tolerance in response to lipopolysaccharide (LPS) and other proinflammatory signals, assessed as defective expression of proinflammatory genes, *IL-12* and tumor necrosis factor-α (*TNF-α*) in particular, and this state is dependent on nuclear overexpression of the p50 NF-κB inhibitory homodimer. We further show in p50

**Note:** A. Saccani, T. Schioppa, C. Porta, and S.K. Biswas equally contributed to this work.

**Requests for reprints:** Antonio Sica, Istituto Clinico Humanitas, via Manzoni, 56, 20089, Rozzano, Milan, Italy. Phone: 39-02-8224-5111; Fax: 39-02-8224-5101; E-mail: antonio.sica@humanitas.it.



doi:10.1158/0008-5472.CAN-06-1867

NF-κB–deficient mice, and in lethally irradiated mice transplanted with $p50^{-/-}$ bone marrow, reversion of the anergic phenotype, delayed tumor progression and increased survival.

## Materials and Methods

**Cell culture.** Peritoneal exudate cells (PEC) and TAMs were incubated in RPMI 1640 containing 10% FCS, 2 mmol/L glutamine, and 100 units/mL penicillin-streptomycin. For the different treatments (stated in the text), we used the following concentrations: IFN-γ, 100 units/mL; LPS, 100 ng/mL; CD40 (to induce activation, TAMs were cocultured for 48 hours with CD40L-transfected J558L cells at 5:1 ratio; ref. 22); TNF-α, 20 ng/mL; IL-1β, 20 ng/mL; IL-10, 20 ng/mL; prostaglandin $E_2$ ($PGE_2$), $10^{-5}$ mol/L. Murine recombinant IFN-γ was kindly donated by Dr. G. Garotta (Roche, Basilea, Switzerland). IL-1β was a gift of Dr. Boraschi (Dompè, L'Aquila, Italy); TNF was from BASF/Knoll (Ludwighafen, Germany); LPS (E. Coli 055:B5) was purchased from Difco (Detroit, MI); IL-10 from Schering-Plough (Kenilworth, NJ); transforming growth factor-β (TGF-β) was from Peprotech (London, United Kingdom); and $PGE_2$ was from Sigma (St. Louis, MO).

**Preparation of PECs and TAMs.** The study was reviewed and approved by the Istituto di Ricerche Farmacologiche Mario Negri Animal Care and Use Committee in compliance with the NIH Guide for the Care and Use of Laboratory Animals and EU directives and guidelines. p50-deficient mice were kindly donated by Drs. Michael Karin and Giuseppina Bonizzi (School of Medicine, University of California San Diego, La Jolla, CA). p50-deficient mice were backcrossed for 15 generations to C57/Bl6 background before being used in the experiments. Tumor inoculation and take was carry out as previously described (17). PECs and TAMs were obtained 3 weeks after tumor cells injection and isolated and identified as previously described (23). Experimental evaluation of animal survival had to be interrupted on day 50 for ethical reasons, according to the directives and guidelines for the use and welfare of laboratory animals.

**Preparation of human monocyte-derived macrophages and TAMs from human ovarian cancer.** Human monocytes were separated as previously described (24). Monocyte-derived macrophages were derived from freshly isolated monocytes as described (24). For the preparation of human TAM, solid tumors were collected from untreated patients with histologically confirmed epithelial ovarian carcinoma admitted to the Department of Obstetrics and Gynecology, San Gerardo Hospital (Monza, Italy). All patients had cancer classified as stage II, III, or IV. Purification of TAM from solid tumor and omentum metastasis was done as described previously for murine tumors.

**Bone marrow transplantation.** C57/BL6 mice were lethally irradiated with a total dose of 900 cGy. Two hours later, mice were injected in tail vein with $15 \times 10^6$ of nucleated cells obtained from C57/BL6 $p50^{+/+}$ or $p50^{-/-}$ donors as follows. Bone marrow–derived cells were obtained by flushing the cavity of freshly dissected femurs with saline. Recipient mice received 0.4 mg/mL gentalyn added to the drinking water starting 1 weeks before irradiation and maintained thereafter. At 8 weeks after bone marrow transplantation (BMT), $10^4$ tumor cells were injected i.m. in the left hind limb of chimeric mice. After 3 weeks of experimental period, to verify engraftment, DNA extracted from PECs of BMT mice was analyzed by PCR for *p50* locus.

**ELISA.** Determination of murine IL-12 and IFN-γ in the cell supernatants was carried out by using ELISA kits purchased from R&D System, Inc. (Minneapolis, MN).

**Real-time PCR.** Cells were cultured in medium alone or supplemented with the indicated agents, and total RNA was purified and analyzed as described (23). Briefly, reverse transcription reaction from 1 μg RNA template was done using Taqman reverse transcription reagents (Applied Biosystems, Piscataway, NJ) as per manufacturer's instructions. Real-time PCR was done using SyBr Green PCR Master Mix (Applied Biosystems, Piscataway, NJ) and detected by ABI-Prism 5700 Sequence Detector (Applied Biosystems, Foster City, CA). Data were processed using the GeneAmp software (Applied Biosystems, Foster City, CA) and normalized by actin gene expression levels. All real-time results were expressed as fold changes in mRNA expression with respect to the control cells. All results were normalized to the expression of the housekeeping gene *β-actin* in the PCR reactions. Data represented are from three independent experiments done in triplicate.

**Immunostaining for p50 NF-κB and laser confocal microscopy.** PECs or TAMs were grown on sterile glass coverslips at a concentration of $2 \times 10^5$ per coverslip in a final volume of 1 mL complete RPMI. Confocal microscopy analysis for the p50 and p65 NF-κB was carried out as previously described (23).

**Immunohistochemical analysis of tumor infiltrating macrophages.** Frozen sections from five wild-type (wt) and five knockout (KO) neoplastic mouse tissues were used for immunohistochemical evaluations. Immunohistochemistry was done using the following antibodies: F4/80 monoclonal antibody (clone C1:A3-1; dilution of 1:50), anti-CD4 (clone 6K1.5; undiluted), and anti-CD8 (clone TIB; dilution 1:5). The sections were rehydrated with PBS and then incubated with primary antibodies for 1 hour. The reactions were revealed by means of an indirect immunoperoxidase technique, with 3,3′-diaminobenzidine free base as chromogen. A quantitative evaluation of immunostaining was applied by using WinRec Program (Image Pro Plus, Media Cybernetics, Silver Spring, MD) and by counting immunopositive cells (identified by the presence of a brown staining) in 10 randomly selected high power fields for each case.

**Western blot analysis.** The nuclear and cytosolic extracts were analyzed by SDS/PAGE (10% acrylamide) as described (23). Immunoblotting was done with rabbit anti-p50 (#1141), anti-p65 (#1226) antisera (25), or by phospho-IκBα antibody (Santa Cruz Biotechnology, Santa Cruz, CA); MyD88 antibody (IMGENEX, San Diego, CA) or actin antibody (Santa Cruz Biotechnology).

**Flow cytometric analysis.** Macrophages were stained using monoclonal antibodies: R. phycoerythrin–conjugated anti-F4/80 (AbD Serotec, Oxford, United Kingdom), allophycocyanin-conjugated anti-TLR2 (eBioscience, San Diego, CA), Alexa Fluor 488 conjugated anti-TLR4 (eBioscience), and their relative isotype controls according to the manufacturer's instructions. Detectors were set to logarithmic amplification, and 10,000 events were analyzed using BD DIVA software. All samples were processed using BD FACS CANTO flow cytometer. Natural killer (NK) cells were stained by using monoclonal anti-NK-1.1 antibody (BD Biosciences, PharMingen, San Diego, CA).

**Electrophoretic mobility shift assay.** Nuclear proteins were prepared and analyzed as described (17). Oligonucleotides were purchased from Life Technologies (Milan, Italy). An IL-6κB double-strand oligonucleotide was used in electrophoretic mobility shift assay (EMSA) as previously reported (26). The following antisera were used in supershift analysis: #1157, raised against the human and murine p50 NF-κB (25); #1226, raised against the human and murine p65 (25); #1266, raised against the murine c-Rel (25).

**Transient transfection.** Transfections were done using Effectene Transfection Reagents (Qiagen, Milan, Italy). Plasmid containing the IL-12p40 promoter linked to the luciferase reporter gene was obtained from Dr. Stephen Male (Howard Hughes Medical Institute and Department of Microbiology, Immunology and Genetics, University of california, Los Angeles, CA). The cytomegalovirus (CMV) construct expressing the murine p50 NF-κB subunit was a kind gift of Dr. Howard Young (National Cancer Institute, Frederick, MD). The total amount of DNA transfected in the different groups was normalized with the empty CMV construct. Luciferase reporter assays were done in 96-well optiplates (Packard Instrument, Inc., Meriden, CT) using the luciferase assay system (Promega, Inc., Madison, WI) according to the manufacturer's instructions.

## Results

**Defective expression of inflammatory cytokines in TAMs.** In agreement with the transcriptome profile of TAMs from a murine fibrosarcoma, which we recently reported (23), Fig. 1*A* shows the defective expression of a few representative inflammatory cytokine genes (*IL-12p40, IL-12p35, TNF-α*, and *IL-6*) and high levels of the immunosuppressive cytokine IL-10, in LPS-activated TAMs. We rule out possible defects in the expression level of the LPS

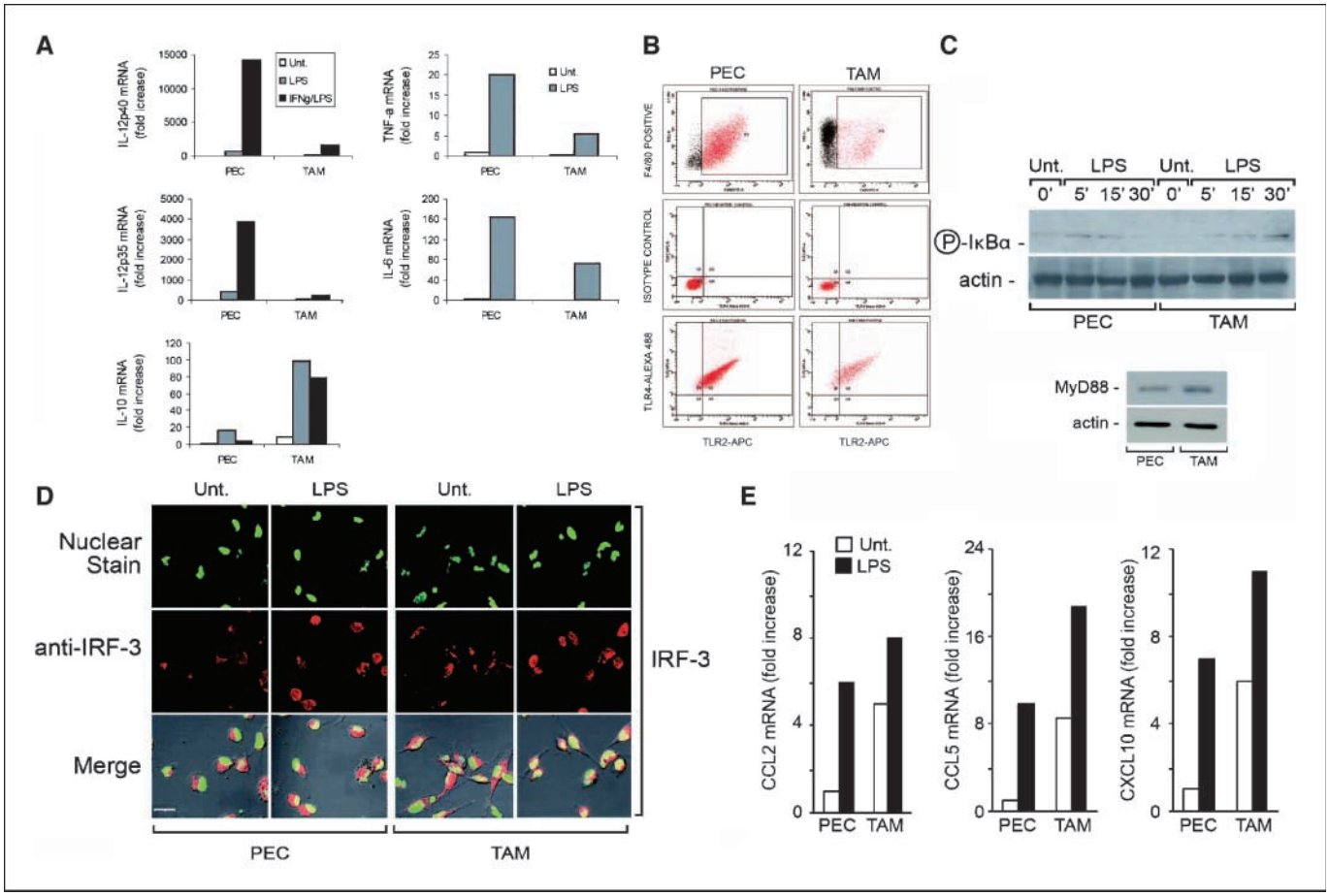


**Figure 1.** Defective expression of NF-κB–dependent cytokine genes in TAMs. *A,* cytokine gene expression in TAMs versus PECs. After isolation of TAMs and PECs, cells were activated for 4 hours with IFN-γ (100 units/mL) and/or LPS (100 ng/mL), as indicated, and total RNA was analyzed by real-time PCR for the expression of the IL-12p40, IL-12p35, TNF-α IL-6, and IL-10 mRNA. *B,* flow cytometric analysis of TLR2/TLR4 expression in PECs and TAMs. Macrophages, identified by positive staining anti-F4/80-PE antibody, were stained with TLR2-APC and TLR4-Alexa 488 antibodies. The populations obtained with isotype-matched antibodies (isotypic control) are shown for comparison. *C, top,* IκBα phosphorylation in TAMs. The cell lysates (20 μg) from untreated or LPS (100 ng/mL)–treated PECs and TAMs for the indicated times were probed with phospho-IκBα antibody. *Bottom,* level of MyD88 protein expression in TAMs versus PECs. Equal loading is visualized by actin expression. *D,* laser confocal microscopic representation of IRF-3 activation in TAMs. Untreated or 2 hours LPS (100 ng/mL)–treated PECs and TAMs were stained for IRF-3 (*red*) or with SYTO for nuclear counterstaining (*green*) and visualized by laser confocal microscopy. IRF-3 staining, nuclear staining, and merge plus phase-contrast images, as indicated. *E,* real-time PCR of CCL2, CCL5, and CXCL10 mRNAs in TAMs and PECs.

receptors TLR2 and TLR4 (27, 28) by showing no significant differences in their *surface* expression level, in TAMs versus PECs (Fig. 1*B*). MyD88, was first characterized as an essential component for the activation of innate immunity by all the TLRs (27). Based on this, we evaluated the level of MyD88 protein in TAMs versus PECs and observed no differences in their respective level of MyD88 protein expression (Fig. 1C). Moreover, to evaluate the functional activity of these receptors, the LPS-dependent phosphorylation of the IκBα inhibitor of NF-κB, an event which precedes NF-κB nuclear translocation (18), was analyzed at different times (Fig. 1*C*). IκBα phosphorylation in TAMs was delayed, thus correlating with the defective expression of NF-κB–dependent cytokine genes.

LPS stimulation of TLR4 promotes activation of an MyD88-dependent and an MyD88-independent pathway (29). The MyD88-dependent pathway controls the events leading to NF-κB activation and to inflammatory cytokine production. The MyD88-independent pathway activates the IFN-regulatory factor (IRF-3) and the late phase of NF-κB activation, leading to the production of IFN-inducible genes. As shown in Fig. 1*D*, IRF-3 nuclear translocation was observed in both PECs and TAMs, suggesting that TAMs are characterized by selective inhibition of the MyD88-dependent pathway, as also substantiated by the observation that LPS-activated TAMs express high levels of the IFN-inducible chemokine genes *CCL2, CCL5*, and *CXCL10* (Fig. 1*E*). These data are in agreement with our previous work showing that TAMs are characterized by enhanced IRF-3/signal transducers and activators of transcription 1 activation (23).

**Nuclear overexpression of the p50 NF-κB inhibitory homodimer in TAMs.** NF-κB is classically described as an heterodimer composed by the p50 and p65 subunits, which drives transcription of a number of inflammatory genes (18). Hence, we investigated the intracellular distribution and DNA-binding activity of NF-κB components in TAMs versus PECs. Strikingly, resting TAMs displayed a massive nuclear localization of the p50 NF-κB protein (Fig. 2*A*). As expected, resting PECs showed low nuclear expression of the p50 NF-κB protein, which was increased by LPS. In a series of four experiments, the ratio of nuclear p50 NF-κB in TAMs versus PECs ranged between 5- and 10-fold. Noteworthy, the level of expression of p50 mRNA were equivalent between PECs and TAMs (data not shown).

Next, we evaluated the kinetics of nuclear translocation of the p50 and p65 NF-κB proteins in LPS-activated TAMs and PECs, as indicated (Fig. 2*B*). Western blot analysis showed a time-dependent increase of nuclear p50 NF-κB in PECs, up to 2 hours, whereas nuclear p50 was constitutively higher in TAMs. In contrast, the LPS-induced nuclear translocation of the p65 NF-κB protein was reduced in TAMs (Fig. 2*A* and *B*) compared with PECs. This result mirrors the delayed LPS-dependent phosphorylation of IκBα observed in TAMs (Fig. 1*C*).

To investigate whether the DNA-binding activity of the NF-κB complexes in TAMs and PECs reflected the intracellular distribution of the p50 and p65 NF-κB subunits, EMSA analysis was done by using nuclear extracts in the presence of a canonical $^{32}$P-dCTP–labeled IL-6 NF-κB double-strand oligonucleotide (Fig. 2*C*). We

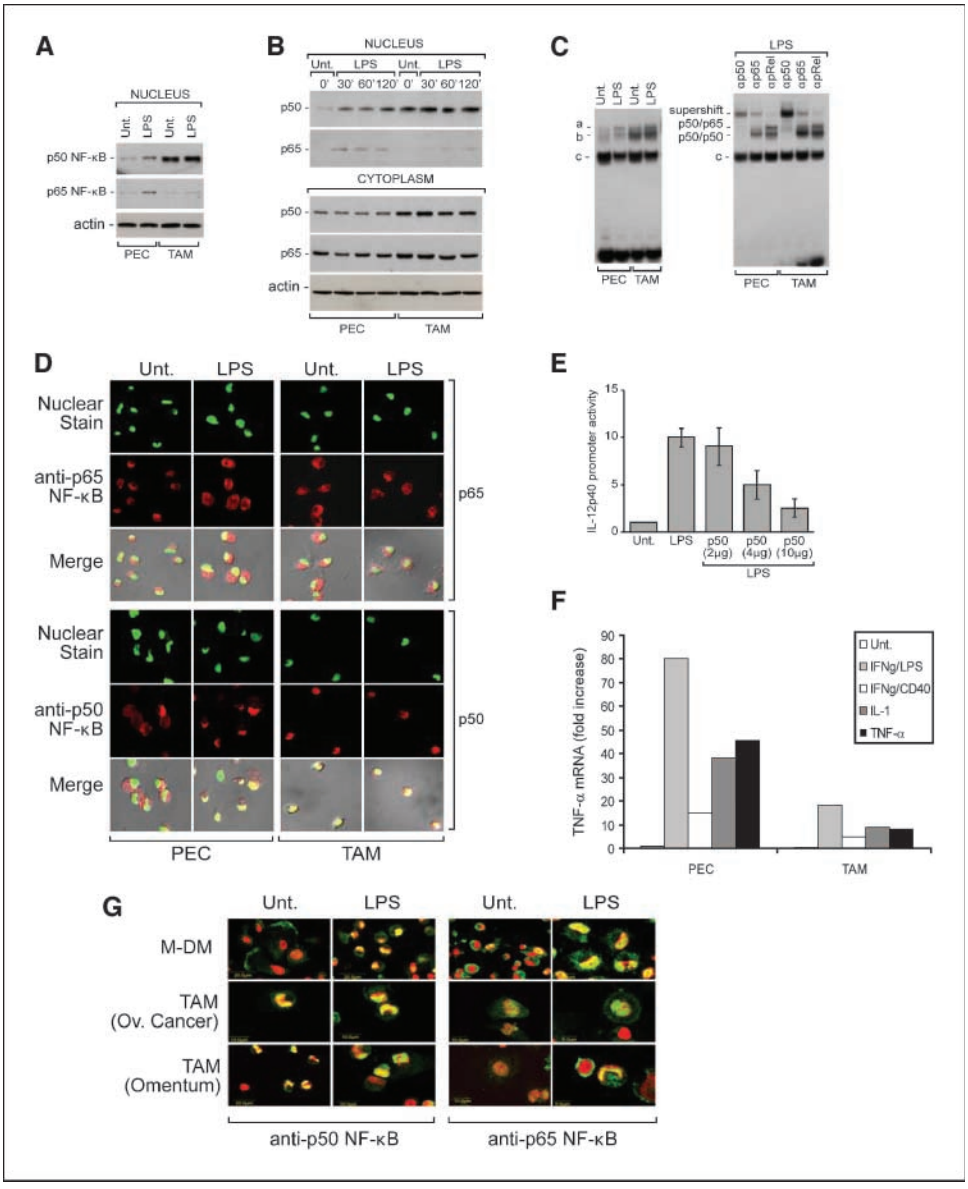


**Figure 2.** Massive nuclear overexpression of the p50 NF-κB inhibitory homodimer in TAMs. *A,* nuclear extracts from untreated and LPS (100 ng/mL) treated PECs and TAMs for 30 minutes were analyzed by Western blot for the p50 and p65 NF-κB proteins. *B,* Western blot and kinetic of nuclear translocation of the p50 and p65 NF-κB subunits in PECs and TAMs. *C,* EMSA analysis of NF-κB complexes expressed in TAMs and PECs. *Left,* nuclear extracts from untreated or LPS-treated (2 hours) PECs and TAMs were used in the presence of the $^{32}$PP-labeled IL-6κB oligonucleotide. *Right,* antisera against the p50, p65 NF-κB subunits, and the cRel transcription factor were used for supershift analysis, as indicated. *D,* laser confocal microscopic representation of p50 and p65 distribution in TAMs. Untreated or 1 hour LPS (100 ng/mL)–treated PECs and TAMs were stained for p50 or p65 as indicated (*red*) or with SYTO for nuclear counterstaining (*green*) and visualized by laser confocal microscopy. *E,* inhibitory effect of p50 overexpression on the IL-12p40 promoter activity. Increasing amounts of the CMVp50 expression vector were cotransfected with 4 μg of the IL-12p40 promoter linked to the luciferase reporter gene in the monocytic cell line RAW 267.4. After 24 hours, the transfected cells were treated with LPS (100 ng/mL). Cells were harvested after another 8 hours and assayed for luciferase activity. Results were normalized for a β-galactosidase activity derived of the CMV-β-Gal expression vector. Fold of induction refers to the level of luciferase-activity in unstimulated RAW 267.4 cells. *Columns,* average of three experiments; *bars,* SE. *F,* reduced expression of TNF-α mRNA level in TAMs activated with different inflammatory stimuli for 4 hours, as indicated. Total RNA from PECs and TAMs was analyzed by real-time PCR for the level of expression of the TNF-α mRNA. Representative of three independent experiments. *G,* laser confocal microscopic representation of p50 and p65 distribution in TAMs from human ovarian carcinoma. Untreated or 2 hours LPS (100 ng/mL)–treated cells were stained for p50 or p65 as indicated (*green*) or with SYTO for nuclear counterstaining (*red*) and visualized by laser confocal microscopy. *M-DM,* monocyte-derived macrophages; *TAM (Ov. Cancer),* TAMs isolated from primary ovarian carcinoma; *TAM (Omentum),* TAMs isolated from omentum metastasis. Results were confirmed in three of three ovarian carcinoma patients.

observed the presence of three DNA/protein complexes (a, b, and c). Although complex a was induced in the nucleus of TAMs and PECs, following LPS treatment for 2 hours, complex b was constitutively expressed in TAMs and was induced at lower level in PECs. Supershift analysis was done to identify the composition of complexes a and b (Fig. 2*C*). An anti-p65 antiserum supershifted only complex a, whereas the antiserum against the p50 NF-κB subunit supershifted both complexes a and b, thus proving that complex a is formed by the p50/p65 heterodimer and complex b by the p50 homodimer. These results confirmed a higher DNA-binding activity of the inhibitory NF-κB p50 homodimer in TAMs compared with PECs. An antiserum against the cRel transcription factor caused only a slight supershift. Complex c, which was equally expressed in PECs and TAMs, was not affected by the presence of the antisera and was not further analyzed.

Activation of NF-κB was also studied in PECs and TAMs by laser confocal microscopy (LCM). Consistent with the biochemical studies, the nuclei of untreated TAMs seemed to contain high constitutive level of p50, whereas in response to LPS, TAMs showed negligible p65 translocation (Fig. 2*D*). Cotransfection of increasing amounts of a p50 NF-κB expression vector with a plasmid containing the IL-12p40 promoter region −350 to +55, encompassing the identified IL-12p40 NF-κB-binding site (30), resulted in a dose-dependent inhibition of the IL-12p40 promoter activity (Fig. 2*E*), in the monocytic cell line RAW 267.4.

Taken together, these results indicate that high expression of the p50 NF-κB subunit in TAMs acts as inhibitory mechanism of gene transcription controlled by NF-κB. To establish whether high p50 NF-κB expression in TAMs could affect other NF-κB–inducing signals (18), we determined the expression of TNF-α mRNA in response to either IFN-γ/LPS, IFN-γ/CD40, TNF-α, or IL-1β. As shown, inducible TNF-α mRNA levels were consistently lower in TAMs compared with PECs (Fig. 2*F*).

To confirm the relevance of this observation in human tumors, TAMs from ovarian carcinoma patients were assayed by LCM for the nuclear translocation of the p50 and p65 NF-κB subunits (Fig. 2*G*). Monocyte-derived macrophages were used as control cell population. Although in monocyte-derived macrophages high levels of nuclear p50 were observed only after activation with LPS, TAMs from both ovarian carcinoma and omentum metastasis displayed constitutive high levels. Higher nuclear levels of p65 NF-κB were induced by LPS in monocyte-derived macrophages compared with TAMs from both the primary tumor and the omentum metastasis. These results are in line with our previous observations on defective production of IL-12p70 by TAMs from human ovarian cancer (17) and were confirmed in three of three ovarian carcinoma patients.

When expressed a high levels, both the RelB and the p52 NF-κB members may act as repressors of the NF-κB transcriptional activity (18). We observed higher nuclear levels of both the RelB and p52 proteins in TAMs compared with PECs (data not shown), suggesting that additional inhibitory mechanisms may take place in TAMs.

**Restoration of TAM responsiveness in p50$^{-/-}$ mice.** To establish whether impaired expression of inflammatory cytokine genes was reversible, TAMs were cultured for different periods under standard conditions and analyzed for cytokine gene expression. After 24 to 72 hours, TAMs recovered their capability to express high levels of IL-12p40 mRNA (Fig. 3*A*) and to secrete the IL-12p70 heterodimer, in response to IFN-γ/LPS (Fig. 3*B*). In addition, IL-10 mRNA expression partially decreased during this period (Fig. 3*A*). TAMs also recovered the capability to express higher TNF-α mRNA levels (Fig. 3*C*). Strikingly, resting TAMs cultured for 24 or 72 hours displayed reduced levels of nuclear p50 NF-κB, comparable with those observed in PECs, and recovered the capability to enhance nuclear p50 NF-κB in response to LPS stimulation (Fig. 3*D*).

p50 mRNA levels were next analyzed in the attempt to investigate the molecular mechanisms guiding nuclear overexpression of p50. Noteworthy, the level of expression of p50 mRNA were equivalent between PECs and TAMs (data not shown). To investigate whether signals present at the tumor microenvironment (15), such as IL-10, TGF-β, $PGE_2$, and TNF-α, could promote DNA-binding activity of the p50 homodimer, nuclear extracts from PEC activated or not, for 36 hours, were analyzed by EMSA (Fig. 3*E*). Although TNF-α induced strong formation of the p50/p65 complex and only a minor activity of the p50 NF-κB homodimer, IL-10, TGF-β, and $PGE_2$ elicited a preferential induction of the p50 NF-κB homodimer.

To definitively assess the role of p50 NF-κB in the LPS-dependent cytokine expression by macrophages, PECs and TAMs obtained from both wt and p50$^{-/-}$ mice were activated for 4 hours and analyzed for the level of IL-12p40 and TNF-α, IL-10, CCL2, and CXCL10 mRNAs. As shown in Fig. 3*F*, p50$^{-/-}$ TAMs expressed higher levels of IL-12p40 and TNF-α mRNAs in response to LPS, comparable with wt PECs. In contrast, lack of p50 NF-κB in TAMs resulted in an appreciable decrease of the LPS-inducible levels of IL-10 mRNA. These observations were confirmed by ELISA (data not shown). Furthermore, LPS-activated p50$^{-/-}$ TAMs expressed higher levels of the IFN-inducible gene *CXCL10* (29).

As the production of inflammatory cytokines by mononuclear phagocytes is essential to promote development of the adaptive immunity and expression of Th1 cytokines by CD4$^+$ T helper lymphocytes (31), splenocytes from wt and p50$^{-/-}$ tumor-bearing mice were tested for the secretion of IFN-γ. As shown in Fig. 3*G*, phorbol 12-myristate 13-acetate/Concanavalin–activated splenocytes from wt tumor bearers (*tum*) secreted lower levels of IFN-γ (4 ng/mL) compared with splenocytes from healthy mice (*N*; 17 ng/mL). Noteworthy, splenocytes from tumor-bearing p50$^{-/-}$ mice significantly recovered their capability to secrete IFN-γ (10.5 ng/mL). To evaluate whether possible changes in the number of IFN-γ-producing NK cells could account for the observed recovery of IFN-γ secretion by splenocytes from p50 KO mice, we determined the number of NK cells in the spleen from wt and p50 KO tumor-bearing mice. As shown (Fig. 3*H*), cytofluorimetric analysis showed no differences in the number of NK cells.

**Tumor growth retardation in p50$^{-/-}$ mice.** Higher expression of inflammatory mediators by p50$^{-/-}$ TAMs suggested possible differences in the level of recruitment of infiltrating leukocytes. Immunohistochemical analysis of serial areas of the MN/MCA1 fibrosarcoma showed similar levels of infiltrating macrophages (F4/80$^+$ cells) in wt versus p50$^{-/-}$ mice (Fig. 4*A*). In contrast, a significant up-regulation of the numbers of CD4$^+$ and CD8$^+$ T lymphocytes was observed in tumors grown in p50$^{-/-}$ mice. This observation is in line with the higher expression of the T cell–specific chemokine CXCL10 observed in p50$^{-/-}$ TAMs (Fig. 3*F*).

To establish whether p50 NF-κB–mediated tolerance in TAMs could play a role in the control of tumor growth, C57B1/6 wt and p50$^{-/-}$ mice were implanted with the MN/MCA-1 fibrosarcoma. Throughout the entire experimental period (3 weeks) tumor growth in p50$^{-/-}$ mice was significantly reduced (Fig. 4*B*). In addition, we monitored the growth rate of the B16 melanoma as we previously showed that TAMs from this tumor share defective IL-12 and

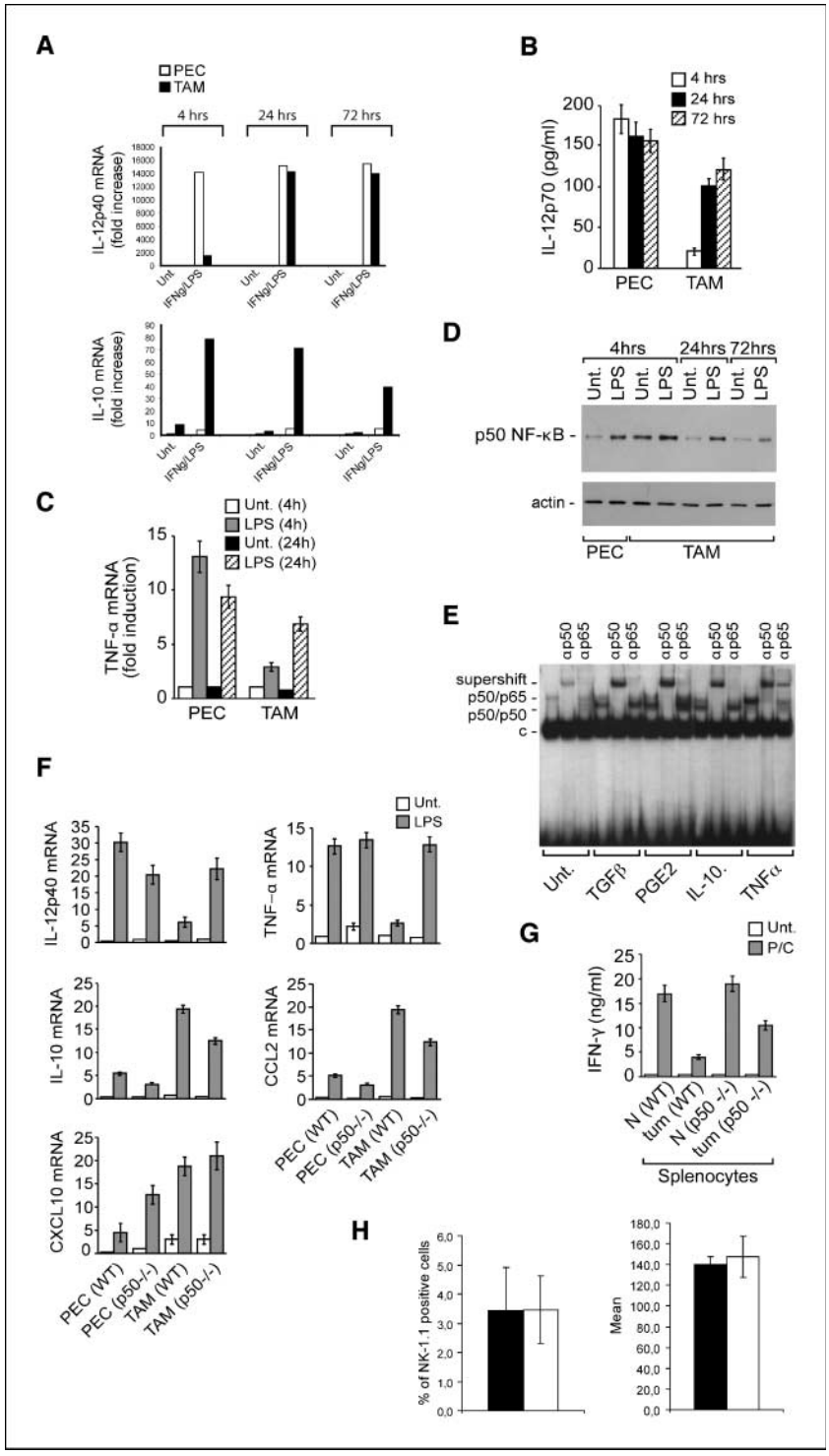


**Figure 3.** Restoration of the LPS responsiveness in isolated TAMs correlates with reduction of p50 NF-κB protein level. *A,* after isolation of TAMs and PECs, cells were cultured for the indicated periods in RPMI and subsequently activated for 4 hours with combination of IFN-γ (100 units/mL) and LPS (100 ng/mL) or LPS alone, as indicated. Expression of the *IL-12p40* and *IL-10* genes was analyzed by real-time PCR. *B,* supernatants from TAMs and PECs stimulated for different times, as indicated, were analyzed by ELISA for IL-12p70 protein secretion. Samples were determined in triplicate. *Columns,* average of three separated experiments; *bars,* SE. *C,* total RNA from TAMs and PECs stimulated for 4 hours, as indicated, were analyzed by real-time PCR for TNF-α mRNA expression. *D,* after isolation of TAMs and PECs, cells were cultured for the indicated periods in standard conditions and subsequently activated for 1 hour with LPS (100 ng/mL). Nuclear extracts were than analyzed by Western blot for the level of the p50 NF-κB subunit. *E,* selected tumor microenvironmental signals preferentially inducing p50 NF-κB homodimer DNA-binding activity. Nuclear extracts from PECs untreated or treated (36 hours) with $10^{-5}$ mol/L $PGE_2$ or 20 ng/mL of the indicated cytokines (TGF-β, IL-10, and TNF-α) were incubated with $^{32}$P-labeled IL6-κB oligonucleotide in the absence or presence of antisera against the p65 or the p50 NF-κB subunits. Thereafter, NF-κB complexes were analyzed by EMSA. *F,* restoration of IL-12p40 and TNF-α mRNA expression in $p50^{-/-}$ TAMs. Total RNA from resting and activated (4 hours) TAMs and PECs were analyzed by real-time PCR for IL-12p40, TNF-α, IL-10, CCL2, and CXCL10 gene expression, as indicated. *G,* restoration of IFN-γ secretion by splenocytes from p50 NF-$\kappa B^{-/-}$ tumor-bearing mice. Splenocytes were treated with phorbol 12-myristate 13-acetate (10 ng/mL) and Concanavalin (1 μg/mL). After 18 hours, supernatants were collected and tested for the presence of IFN-γ by ELISA. Supernatants from eight mice, from each group, were analyzed. *Columns,* average of three independent experiments; *bars,* SE. *H,* flow cytometric analysis of NK cells in the spleen from tumor bearing wt and p50 KO tumor bearing mice. NK cells were identified by positive staining with anti-NK-1.1 antibody. Percentage of positive NK-1.1 cells and the mean of fluorescence. Five wt and five p50 KO mice were analyzed.

enhanced IL-10 phenotype (17). In agreement, a significant reduction of B16 tumor growth was observed in $p50^{-/-}$ mice (Fig. 4*C*). Accordingly, the survival of $p50^{-/-}$ mice was prolonged with 6 of 10 $p50^{-/-}$ mice (60%) alive on day 50, when all wt controls had died with a median survival of 42 days ($P < 0.01$). Finally, to test whether tumor growth retardation observed in p50-deficient mice could be ascribed to the absence of p50 in hematopoietic cells, bone marrow from either wt or $p50^{-/-}$ mice was transplanted in lethally irradiated C57/Bl6 wt mice. As shown in Fig. 4*D*, mice transplanted with $p50^{-/-}$ bone marrow displayed reduced tumor growth, similar to what observed in $p50^{-/-}$ mice.

## Discussion

The presence of inflammatory cells in solid tumors has long suggested that cancers arise at sites of chronic inflammation (1),

and recent molecular confirmations in inflammation-associated cancer models (4–6) support a causal relationship between NF-κB–mediated inflammation and tumorigenesis. Here, we confirm and extend previous observations (17) that TAMs have defective activation of NF-κB in response to different agonists (LPS, CD40L, TNF-α, and IL-1β). The defect of TAMs was selective, in that the activation by LPS of MyD88-independent IRF-3 was normal, and TAMs produced copious amounts of IL-10 and chemokines downstream of this pathway. Defective M1 activation of TAMs was associated with elevated nuclear localization of p50 homodimers. Finally, TAMs isolated from tumors transplanted in $p50^{-/-}$ deficient mice showed essentially normal M1 activation, associated with significant tumor growth retardation. Bone marrow chimeras reconstituted with $p50^{-/-}$ hematopoietic cells showed reduced tumor growth, suggesting that indeed mononuclear phagocyte activity is a major player in growth retardation. These results indicate that p50 plays a pivotal role in tuning NF-κB–dependent M1 activation of TAMs and in the subversion of macrophage responsiveness in established neoplasia.

Increased p50 NF-κB expression is functionally associated with the LPS-induced tolerance of macrophages (32), and peritoneal macrophages from $p50^{-/-}$ mice have been shown to be incapable of undergoing endotoxin tolerance-mediated suppression of TNF-α production (33). We observed that TAMs from $p50^{-/-}$ tumor-bearing mice displayed normal expression of IL-12 and TNF-α, an event paralleled by decreased tumor growth and increased animal survival. Although during bacterial infection, or sepsis, up-regulation of the p50 NF-κB homodimer is an adaptive response providing protection from pathologic hyperactivation of the innate immune system (33), our results suggest that cancer may exploit this mechanism to impair type 1 inflammation and effective activation of adaptive Th1 immunity. In support of this and in agreement with previous reports (31, 33, 34), we observed that overexpression of the p50 NF-κB subunit in the monocytic cell line RAW 267.4 results in the inhibition of the IL-12p40 promoter transcriptional activity. Moreover, TAMs cultured in standard conditions for a period of 24 to 72 hours reduced their level of p50 NF-κB protein to physiologic levels and recovered their capability to express IL-12p70 and TNF-α. Thus, the unique phenotype of TAMs is induced by the tumor microenvironment and overexpression of p50 NF-κB in these cells, and possibly in other components of the immune system, drives inhibition of immune functions in cancer bearers. Constitutive nuclear overexpression of the p50 NF-κB was also observed in TAMs from human ovarian cancer, that are characterized by defective IL-12p70 production (17). NF-κB seems a main target of tumor-mediated immune dysfunction observed in cancer bearers. It was reported that anergic T cells from cancer bearers display defective NF-κB

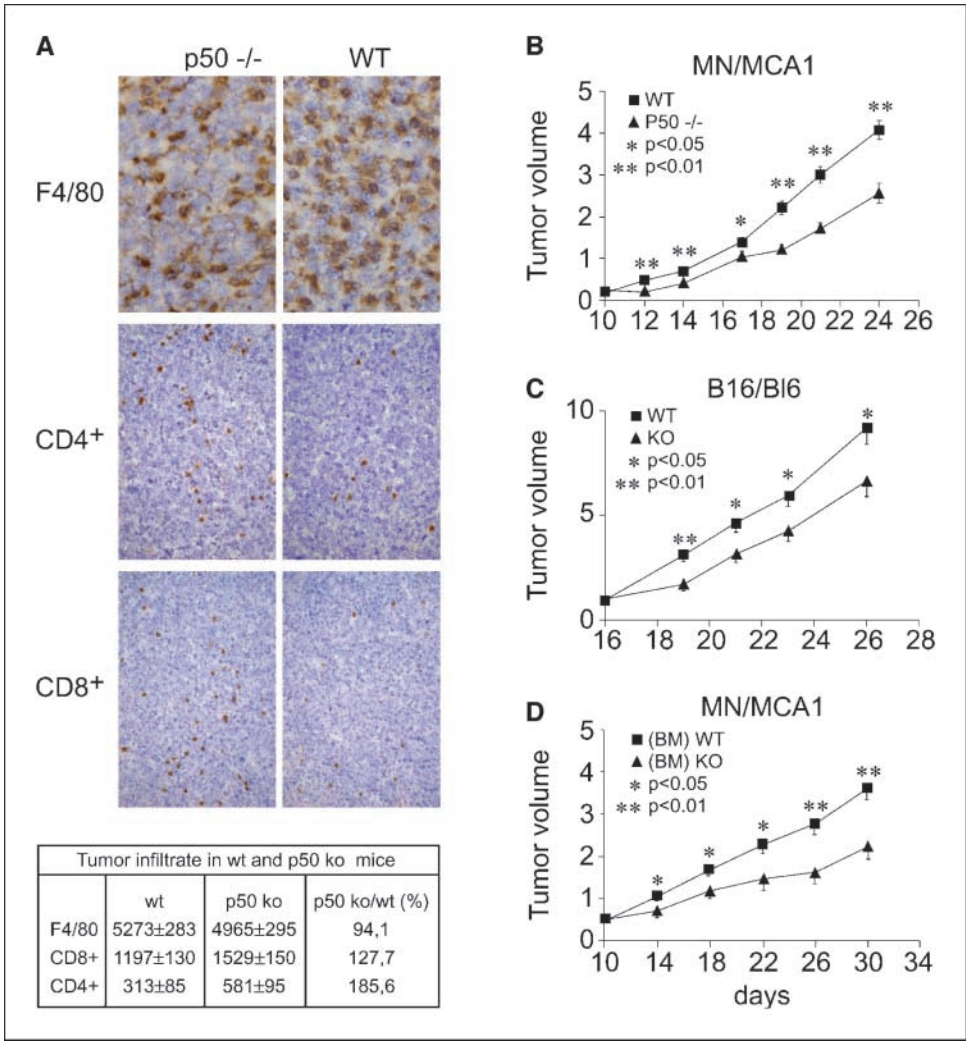


| Tumor infiltrate in wt and p50 ko mice | | | |
|---|---|---|---|
| | wt | p50 ko | p50 ko/wt (%) |
| F4/80 | 5273±283 | 4965±295 | 94,1 |
| CD8+ | 1197±130 | 1529±150 | 127,7 |
| CD4+ | 313±85 | 581±95 | 185,6 |

**Figure 4.** *A,* cells count of histologic sections of the MN/MCA1 tumor from normal and p50 NF-κB–deficient mice. F4/80, macrophages; $CD8^+$, $CD8^+$ T lymphocytes; $CD4^+$, $CD4^+$ T lymphocytes. Positive cells were identified by the brown staining of the cytoplasmic membrane (immunostaining, 3,3′-diaminobenzidine; original magnification, ×20). *B,* growth inhibition of the MN/MCA1 fibrosarcoma in p50 NF-κB–deficient mice. *C,* growth inhibition of the B16 melanoma in p50 NF-κB–deficient mice. *D,* growth inhibition of the MN/MCA1 fibrosarcoma in chimeric mice obtained by transplanting bone marrow of donor $p50^{-/-}$ mice in lethally irradiated C57/BL6 WT recipient mice. Tumor volume was measured twice a week with calipers, and tumor volume ($cm^3$) was estimated by the formula for ellipsoid: (length × $width^2$/2). *Points,* mean of 10 tumors; *bars,* SE.

activation (35) and Th1 response (36), and that *in vivo* anergized T cells express a predominant formation of the p50 NF-κB inhibitory homodimer, likely responsible for repression of cytokine expression (37).

The mechanisms controlling p50 biogenesis have been elucidated in part. Lin et al. have shown that cotranslational folding of the $NH_2$-terminal portion of p105 protects this region that forms p50 from degradation by proteasome (38). In addition, the p50 NF-κB activity is also controlled by Bcl3, a close homologue of IκB proteins (39), which displays versatile functions, including cytoplasmic activation of p50 homodimers and their nuclear translocation and modulation of the NF-κB activity in the nucleus (39–42). Interestingly, it was observed that IL-10 selectively induces nuclear translocation and DNA binding of p50/p50 homodimers in human monocytic cells (43). This well correlates with our previous observation of high production of IL-10 by TAMs of the MN/MCA1 fibrosarcoma, which we reported *in vitro* (17) and *in vivo* (23). Moreover, our data also show that in addition to IL-10, $PGE_2$ and TGF-β, which are expressed by TAMs (7) and promote M2-type polarized inflammation (15), are microenvironmental signals promoting p50 NF-κB homodimer activity. Of interest, $PGE_2$ was shown to mimic the phenotype of TAMs, being able to enhance p50 and inhibit p65 translocation and DNA-binding activity (44). Of interest, peritoneal macrophages from tumor-bearing mice were impaired in the p65 NF-κB nuclear translocation (45).

We observed that TAMs from $p50^{-/-}$ mice express higher level of the T-cell recruiting and IFN-inducible chemokine CXCL10 (22, 29, 46, 47), which correlates with increased infiltration of $CD4^+$ and $CD8^+$ T lymphocytes in tumors from $p50^{-/-}$ mice. This observation is in line with the established antitumor role of these cells as well as with inhibition of tumor growth and increased survival of $p50^{-/-}$ mice.

Overall, our data indicate that the tumor microenvironment tolerates macrophages by inducing high nuclear localization of the p50 NF-κB inhibitory homodimer. This observation is consistent with previous results in mouse and human tumors (7, 17), whereas it seems in contrast with recent results showing a key role of the NF-κB pathway in liver and colon carcinogenesis (4, 5). In particular, lineage-restricted inactivation of IKKβ revealed a nonreduntant role of NF-κB activation in myeloid cells in colon carcinogenesis (5), an observation generally consistent with a protumor function of inflammatory reactions and TAMs in particular (1–3). We speculate that the apparent discrepancy between results reported here of detective p50 homodimer-driven NF-κB activation in TAMs and these recent observations (4, 5) reflects differential involvement of NF-κB–driven full-blown inflammation in early steps of carcinogenesis compared with established neoplasia. Although NF-κB activation in myeloid cells would facilitate the early steps of carcinogenesis, tumor-mediated increased expression of p50 NF-κB in TAMs would guide smoldering inflammation and progression of established neoplasia. Inhibition of p50 NF-κB expression in TAMs may represent an innovative anticancer strategy, complementary to immunostimulatory strategies.

## Acknowledgments

Received 5/23/2006; revised 8/9/2006; accepted 9/27/2006.

**Grant support:** Associazione Italiana Ricerca sul Cancro (AIRC), Italy; European Community; Ministero Istruzione Università Ricerca, Italy; Istituto Superiore Sanita; Alfredo Leonardi fellowship (S.K. Biswas); G.L. Pfeiffer foundation (S.K. Biswas); and AIRC fellowship (C. Porta).

The costs of publication of this article were defrayed in part by the payment of page charges. This article must therefore be hereby marked *advertisement* in accordance with 18 U.S.C. Section 1734 solely to indicate this fact.

We thank Andrea Doni for technical assistance with laser confocal microscopy, Mariella Parenza for preparing mice chimeras, and Drs. Michael Karin and Giuseppina Bonizzi for the kind gift of the p50 NF-κB–deficient mice.

## References

1. Balkwill F, Mantovani A. Inflammation and cancer: back to Virchow? Lancet 2001;357:539–45.
2. Coussens LM, Werb Z. Inflammation and cancer. Nature 2002;420:860–7.
3. Balkwill F, Charles KA, Mantovani A. Smoldering and polarized inflammation in the initiation and promotion of malignant disease. Cancer Cell 2005;7:211–7.
4. Pikarsky E, Porat RM, Stein I, et al. NF-κB functions as a tumour promoter in inflammation-associated cancer. Nature 2004;431:461–6.
5. Greten FR, Eckmann L, Greten TF, et al. IKKβ links inflammation and tumorigenesis in a mouse model of colitis-associated cancer. Cell 2004;118:285–96.
6. de Visser KE, Korets LV, Coussens LM. *De novo* carcinogenesis promoted by chronic inflammation is B lymphocyte dependent. Cancer Cell 2005;7:411–23.
7. Mantovani A, Sozzani S, Locati M, Allavena P, Sica A. Macrophage polarization: tumor-associated macrophages as a paradigm for polarized M2 mononuclear phagocytes. Trends Immunol 2002;23:549–55.
8. Bottazzi B, Polentarutti N, Acero R, et al. Regulation of the macrophage content of neoplasms by chemoattractants. Science 1983;220:210–2.
9. Matsushima K, Larsen CG, DuBois GC, Oppenheim JJ. Purification and characterization of a novel monocyte chemotactic and activating factor produced by a human myelomonocytic cell line. J Exp Med 1989;169:1485–90.
10. Yoshimura T, Robinson EA, Tanaka S, Appella E, Kuratsu J, Leonard EJ. Purification and amino acid analysis of two huan glioma-derived monocyte chemoattractants. J Exp Med 1989;169:1449–59.
11. Mantovani A, Bottazzi B, Colotta F, Ruco L. The origin of tumor-associated macrophages. Immunol Today 1992;13:265–70.
12. Gordon S. Alternative activation of macrophages. Nat Rev Immunol 2003;3:23–35.
13. Anderson CF, Mosser DM. A novel phenotype for an activated macrophage: the type 2 activated macrophage. J Leukoc Biol 2002;72:101–6.
14. Goerdt S, Orfanos CE. Other functions, other genes: alternative activation of antigen-presenting cells. Immunity 1999;10:137–42.
15. Mantovani A, Sica A, Sozzani S, Allavena P, Vecchi A, Locati M. The chemokine system in diverse forms of macrophage activation and polarization. Trends Immunol 2004;25:677–86.
16. Mantovani A, Sica A, Locati M. Macrophage polarization comes of age. Immunity 2005;23:344–6.
17. Sica A, Saccani A, Bottazzi B, et al. Autocrine production of IL-10 mediates defective IL-12 production and NF-κ B activation in tumor-associated macrophages. J Immunol 2000;164:762–7.
18. Bonizzi G, Karin M. The two NF-κB activation pathways and their role in innate and adaptive immunity. Trends Immunol 2004;25:280–8.
19. Makarov SS. NF-κB as a therapeutic target in chronic inflammation: recent advances. Mol Med Today 2000;6:441–8.
20. Chouaib S, Asselin-Paturel C, Mami-Chouaib F, Caignard A, Blay JY. The host-tumor immune conflict: from immunosuppression to resistance and destruction. Immunol Today 1997;18:493–7.
21. Adib-Conquy M, Adrie C, Moine P, et al. NF-κB expression in mononuclear cells of patients with sepsis resembles that observed in lipopolysaccharide tolerance. Am J Respir Crit Care Med 2000;162:1877–83.
22. Akira S, Sato S. Toll-like receptors and their signaling mechanisms. Scand J Infect Dis 2003;35:555–62.
23. Biswas SK, Gangi L, Paul S, et al. A distinct and unique transcriptional programme expressed by tumor-associated macrophages: defective NF-[κ]B and enhanced IRF-3/STAT1 activation. Blood 2006;107:2112–22.
24. Allavena P, Piemonti L, Longoni D, et al. IL-10 prevents the differentiation of monocytes to dendritic cells but promotes their maturation to macrophages. Eur J Immunol 1998;28:359–69.
25. Rice NR, MacKichan ML, Israel A. The precursor of NF-κ B p50 has I κ B-like functions. Cell 1992;71:243–53.
26. Saccani S, Varesio L, Ghosh P, Sica A. Divergent effects of Dithiocarbamates on AP-1 containing and AP-1 less NFAT sites. Eur J Immunol 1999;29:1194–201.
27. Takeda K, Kaisho T, Akira S. Toll-like receptors. Annu Rev Immunol 2003;21:335–76.
28. Tsan MF, Gao B. Endogenous ligands of Toll-like receptors. J Leukoc Biol 2004;76:514–9.
29. Akira S, Takeda K. Toll-like receptor signaling. Nat Rev 2004;4:499–511.
30. Murphy TL, Cleveland MG, Kulesza P, Magram J, Murphy KM. Regulation of interleukin 12 p40 expression through an NF-κ B half-site. Mol Cell Biol 1995;15:5258–67.
31. Trinchieri G. Interleukin-12 and the regulation of innate resistance and adaptive immunity. Nat Rev Immunol 2003;3:133–46.
32. Ziegler-Heitbrock HW, Petersmann I, Frankenberger M. p50 (NF-κ B1) is upregulated in LPS tolerant P388D1 murine macrophages. Immunobiology 1997;198:73–80.
33. Bohuslav J, Kravchenko VV, Parry GC, et al. Regulation of an essential innate immune response by the p50 subunit of NF-κB. J Clin Invest 1998;102:1645–52.

**34.** Liu J, Beller D. Aberrant production of IL-12 by macrophages from several autoimmune-prone mouse strains is characterized by intrinsic and unique patterns of NF-κ B expression and binding to the IL-12 p40 promoter. J Immunol 2002;169:581–6.

**35.** Ghosh P, Sica A, Young HA, et al. Alteration in NF-κB/Rel family proteins in splenic T cells from tumor-bearing mice and reversal following therapy. Cancer Res 1994;54: 2969–872.

**36.** Ghosh P, Komschlies LK, Cippitelli M, et al. Gradual loss of T-helper 1 population in spleen of mice during progressive tumor growth. J Natl Cancer Inst 1995;87: 1478–83.

**37.** Sundstedt A, Sigvardsson M, Leanderson T, Hedlund G, Kalland T, Dohlsten M. *In vivo* anergized $CD4^+$ T cells express perturbed AP-1 and NF-κ B transcription factors. Proc Natl Acad Sci U S A 1996; 93:979–84.

**38.** Lin L, DeMartino N. Cotranslational biogenesis of NF-κB p50 by the 26S proteasome. Cell 1998;92: 819–28.

**39.** Franzoso G, Bours V, Park S, Tomita-Yamaguchi M, Kelly K, Siebenlist U. The candidate oncoprotein Bcl-3 is an antagonist of p50/NF-κ B-mediated inhibition. Nature 1992;359:339–42.

**40.** Bours V, Franzoso G, Azarenko V, et al. The oncoprotein Bcl-3 directly transactivates through κ B motifs via association with DNA-binding p50NF-κB homodimers. Cell 1993;5:729–39.

**41.** Watanabe N, Iwamura T, Shinoda T, Fujita T. Regulation of NFKB1 proteins by the candidate oncoprotein BCL-3: generation of NF-κB homodimers from the cytoplasmic pool of p50–105 and nuclear translocation. EMBO J 1997;12:3609–20.

**42.** Lenardo M, Siebenlist U. Bcl-3-mediated nuclear regulation of the NF-κ B *trans*-activating factor. Immunol Today 1994;4:145–7.

**43.** Driessler F, Venstrom K, Sabat R, Asadullah K, Schottelius AJ. Molecular mechanisms of interleukin-10-mediated inhibition of NF-κB activity: a role for p50. Clin Exp Immunol 2004;135:64–73.

**44.** Gomez PF, Pillinger MH, Attur M, et al. Resolution of inflammation: prostaglandin E2 dissociates nuclear trafficking of individual NF-κB subunits (p65, p50) in stimulated rheumatoid synovial fibroblasts. J Immunol 2005;175:6924–30.

**45.** Torroella-Kouri M, Ma X, Perry G, et al. Diminished expression of transcription factors nuclear factor κB and CCAAT/enhancer binding protein underlies a novel tumor evasion mechanism affecting macrophages of mammary tumor-bearing mice. Cancer Res 2005;65:10578–84.

**46.** Hertzog PJ, O'Neill LA, Hamilton JA. The interferon in TLR signaling: more than just antiviral. Trends Immunol 2003;24:534–9.

**47.** Moser B, Wolf M, Walz A, Loetscher P. Chemokines: multiple levels of leukocyte migration control. Trends Immunol 2004;25:75–84.